Model for the Leading Waves of Tsunamis

Srinivas Tadepalli
Department of Mechanical Engineering, Stanford University, Stanford, California 94305-3030

Costas Emmanuel Synolakis
School of Engineering, University of Southern California, Los Angeles, California 90089-2531
(Received 2 August 1995; revised manuscript received 13 May 1996)

We propose a model for the leading wave of tsunamis to explain why although the coastal manifestation of a tsunami is assumed solitary-wave-like it is most often accompanied by a shoreline which recedes first before advancing up the beach, suggesting a leading-depression N-wave. Far field, we use the Korteweg–de Vries equation, and find that N-waves of geophysical scale do not fission over transoceanic propagation distances. Near shore, we use shallow-water theory to calculate the evolution and runup of emerging non-breaking waves, and observe that they evolve according to Green's law. We discuss the effects of certain ground deformation parameters and provide one application by modeling the Nicaraguan tsunami of 1 September 1992. [S0031-9007(96)01008-3]

PACS numbers: 91.30.Nw, 92.10.Fj, 92.10.Hm

Recent earthquakes in Nicaragua (1 September 1993), Flores, Indonesia (12 December 1992), Okushiri, Japan (7 July 1993), East Java, Indonesia (6 June 1994), Kuril Islands, Russia (4 October 1994), Mindoro, Philippines (14 November 1994), Manzanillo, Mexico (9 October 1995), and Chimbote, Peru (21 February 1996) have produced tsunami waves which caused nearby shorelines to first recede before advancing. These observations have challenged further the prevailing paradigm for studying the coastal effects of tsunamis, i.e., the canonical model of a Boussinesq solitary wave profile propagating over constant depth and then climbing up a sloping beach [1]. To quantify the persistent field observations and tsunami folklore, a class of water waves referred to as N-waves has been proposed [2] for near-shore–generated tsunamis, and it was observed that at least for three different types of N-waves, leading-depression N-waves climb up higher on sloping beaches than leading-elevation N-waves with the same leading-wave amplitude. The utility of these runup laws [2] was recently demonstrated by Geist [3] to supplement numerical computations for a Cascadia subduction zone type giant earthquake. However, unresolved questions persist as to the long-distance hydrodynamic stability of these waves. Also, given the uncertainty associated with inferring the sea-bottom displacement from distant strong-motion records [4], there is little understanding as to the relative effects of the vertical deformation, of the deformed area, or of the relative magnitudes of subsidence and uplift, forcing laboratory modelers to work exclusively with solitary waves or periodic long waves, and numerical modelers to routinely introduce arbitrary large "amplification" factors to fit their results to runup field observations.

We will attempt to address these questions here by first deriving an initial sea-surface profile for the leading wave of a tsunami from a specification of the sea-bottom deformation and by demonstrating that this profile encompasses as special cases all N-wave-like and solitary-wave-like profiles used in earlier studies [2,3,5,6]. We then will discuss their stability with respect to fission in far-field evolution. We will then derive near-shore evolution relationships and we will obtain certain asymptotic estimates of the relative effects of some generation parameters on the runup of non-breaking waves. We therefore propose

$$\eta(x) = \mathcal{E}_g, \mathcal{H}(x - X_2)\,\mathrm{sech}^2[\gamma(x - \theta)]|_{t=0} \quad (1)$$

as a profile for the leading wave of tsunamis. Here $\gamma = \sqrt{3\mathcal{H}p_0/4}$, $\theta = X_1 + ct$, $L = X_1 - X_2$, $c = 1$, and p_0 is a steepness parameter. $\mathcal{E}_g < 1$ is a scaling parameter defining the crest amplitude introduced only for reference to ensure that the waveheight (1) is $\mathcal{H}$; $\mathcal{E}_g$ can be chosen to fit desired field-inferred surface profiles. $\mathcal{H}$ and the wavelength of the profile inferred from (1) are vertical and horizontal measures of the ground deformation, respectively. When the crest and trough heights are equal, we will refer to these N-waves as isosceles [2]; the latter can be described by (1) by setting $L = 0$. As suggested by Carrier [6], multilobe waves similar to (1) can be described by combinations of Gaussian profiles; we prefer (1) because it allows for direct derivation of asymptotic results. Here, for brevity, we will refer to all multilobe tsunamis as N-waves. We will also use the qualifier non-breaking to refer to waves which do not break in the specific evolution problem, and we note that the same leading wave which evolves to its maximum penetration without breaking on a steep beach may break on a gentle beach; in the steepness range of geophysical interest the leading waves of most tsunamis do not break on most natural beaches, but they may break when advancing up rivers, during overland flow, or when focused on headlands.

To motivate the generation of N-waves and our particular choice of the initial profile, consider the linearized shallow-water equation, long believed as the physically

realistic generation approximation [7,8], i.e.,

$$\eta_{tt} - \eta_{xx} = h_{0tt}, \qquad h_0 = -\frac{2\mathcal{E}_g\mathcal{H}}{\gamma}\tanh[\gamma(x-\theta)], \tag{2}$$

where $h_0(x,t)$ is the ground motion, measured from a horizontal datum corresponding to a sudden uplift and/or subsidence of the sea bottom such as would occur with normal thrust fault. In nature, the ground deformation would stop almost immediately after the earthquake and the deformation would not propagate as the definition of h_0 suggests. Nonetheless, since our objective is only to determine an initial profile valid only for short times, the above ground deformation is adequate. It can be verified directly that (1) is an exact solution of (2). Other ground motions [7,8] would also produce multilobe waves, but not of the same mathematical form; the advantage of the ground deformation h_0 in (2) is that it allows for the explicit evaluation of the near-field and far-field effects in terms of simple and intuitive asymptotic formulae.

To appreciate the range of surface profiles that (1) describes, Fig. 1(a) compares a classical Boussinesq solitary-wave profile with the surface profile obtained by (1) and, for reference, with an isosceles leading-elevation (LEN) wave with the same leading wave steepness $p_0 = 1$ and a Gaussian profile [6]. Figure 1(b) shows leading-depression (LDN) profiles generated by Eq. (1) for a fixed $\mathcal{H}$ and different values of L and, for reference, an isosceles LDN and a combination of Gaussian profiles [6].

As an initial condition we will use the N-wave of (1), and then we will solve the Korteweg–de Vries (KdV) equation to calculate transoceanic propagation over constant depth. Once the wave arrives near shore, we will use the shallow-water wave equations [1]; it is well established that for the non-breaking waves we are considering here dispersive effects do not have sufficient time to manifest over the relatively short propagation distances on a sloping beach. We will show that both LDNs and LENs evolve according to a relationship equivalent to Greens' law [9,10]. Finally, we will provide results for the maximum runup and we will discuss the relative importance of certain generation parameters.

Propagation distance for solitary wave evolution.—Since we are most interested in the effective propagation distance over which the leading solitary waves emerge, we propagated LDN waves by solving the KdV equation numerically [11]. No distinct solitary waves emerge when LDN waves with an initial height-to-depth ratio of 0.01 (much larger amplitude than a possible transoceanic tsunami) are propagated through twice typical transoceanic distances of about 4000 depths [see Fig. 2(b)]. LDN waves of the same family, but with geophysically realistic initial height-to-depth ratio of 0.001 were practically unchanged even after propagating over 2000 depths, indicating the hydrodynamic stability of N-waves and perhaps explaining for the first time anecdotal reports of LDN waves striking Hawaii after the Chilean 1960 event.

Runup and coastal evolution of N waves.—We will now solve the propagation problem described by the linearized shallow-water wave equations (SW), $\eta_{tt} - (\eta_x h)_x = 0$ normalized with the offshore depth d as the characteristic length scale, and $\sqrt{g/d}$ as the time scale, $h(x) = x/\cot\beta$, when $x \le \cot\beta$ and $h(x) = 1$ otherwise. It is widely believed that these equations describe the essential physics of the coastal tsunami evolution problem well [1]. When the incident wave from infinity is of the form $\int_{-\infty}^{\infty}\Phi(\omega)e^{i\omega t}\,d\omega$, then the transmitted wave to the beach is given by

$$\eta(x,t) = 2\int_{-\infty}^{\infty}\frac{\Phi(\omega)J_0(2\omega\sqrt{x\cot\beta})e^{-i\omega(\cot\beta+ct)}}{J_0(2\omega\cot\beta) - iJ_1(2\omega\cot\beta)}\,d\omega, \tag{3}$$

where $\Phi(\omega)$ is the transform function of the incoming wave. The amplification factor (kernel) in the above equation was originally obtained by Keller and Keller [12] and can be used directly to calculate the evolution of the wave at any location along the beach; when $x = 0$, $R(t) = \eta(0,t)$ and its maximum value $\mathbf{R}$ is the maximum runup, i.e., the elevation above the shoreline at the point of maximum penetration of the wave. Carrier [8] and Synolakis [5] have proved the runup invariance

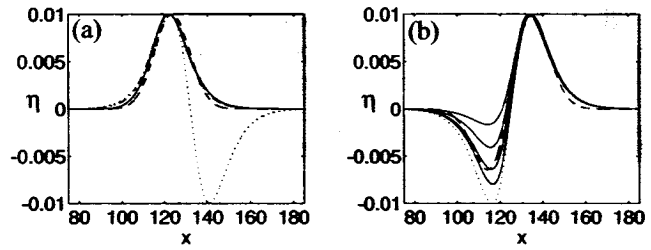

FIG. 1. (a) Comparison of Boussinesq solitary profile (− · −), N-wave solitary profile (—) ($L = 30, \mathcal{E}_g = 0.032$), Gaussian profile (− −) [6], and leading elevation isosceles N-wave (··). (b) A family of leading-depression waves generated by N-wave (—) for $L = 8, 4, 2, 1$ and $p_0 = 1$, combination of Gaussian profiles (− −) [6] and leading-depression isosceles N-wave (··) generated with $L = 0$, $p_0 = 1$.

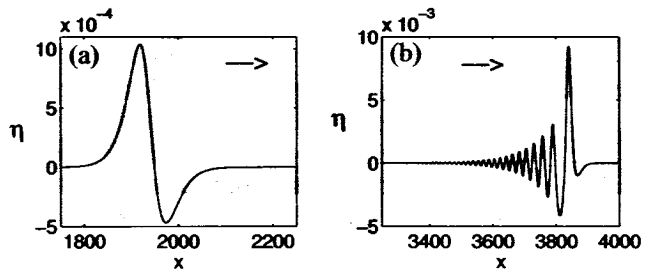

FIG. 2. (a) LDN N-wave generated by Eq. (1) for ($X_1 = 190$, $X_2 = 200$, $\mathcal{H} = 1.E-03$) propagated by KdV to 2000 depths. (b) LDN N-wave generated by Eq. (1) for ($X_1 = 98$, $X_2 = 100$, $\mathcal{H} = 1.E-02$) propagated by KdV to 4000 depths.

between linear and nonlinear theory, and it has been repeatedly shown [13,14] that linear theory describes well the evolution of the maximum height of long waves which offshore had a Boussinesq solitary-wave profile. Therefore, without loss of generality, we will use linear theory calculate the evolution of the waveheight and the maximum runup of non-breaking waves.

The transform $\Phi(\omega)$ of (1) is obtained through contour integration [2] and is given by,

$$\Phi = \frac{2\mathcal{E}_g}{3p_0}\cosh\left(\frac{\pi\omega}{2\gamma}\right) \times \left\{L\omega - i\left[1 - \frac{\pi\omega}{2\gamma}\coth\left(\frac{\pi\omega}{2\gamma}\right)\right]\right\}e^{i\omega X_1} \quad (4)$$

The evolution of this wave is obtained by substituting Eq. (4) into Eq. (3). After using contour integration [15–17] and computing the Laurent expansions we find that

$$\eta(x,t) = \eta_0\left[\gamma d_0 \operatorname{sech}^2(\gamma\phi') + \frac{1}{2}e^{-\gamma\phi'}\operatorname{sech}(\gamma\phi')\right], \quad (5)$$

where $\eta_0 = 4\mathcal{E}_g\gamma_s/(3\sqrt{p_0}h^{1/4})$, $\gamma_s = \sqrt{3\mathcal{H}/4}$, $\phi = X_1 + \cot\beta - ct$, $\phi' = \phi - 2\sqrt{x\cot\beta}$, and $d_0 = L - \phi'$. Note that only η_0 depends on the local depth h. Solving $\partial\eta/\partial\phi' = 0$, the extremum η_{ext} for any location x, we obtain $|\eta_{\text{ext}}(x)/\mathcal{H}| = F(\gamma,\phi'_m)/h^{1/4}$ where ϕ'_m is the phase corresponding to η_{ext}. Therefore for any given initial LEN or LDN wave, η_{ext} is independent of L and depends only on the local depth h on the sloping beach. N-waves are therefore seen to evolve far from the shoreline in a manner similar to what is referred to as Greens' law [9,10,13] whether a leading-depression or leading-elevation wave.

An approximate absolute upper bound for the runup of a non-breaking LDN was calculated earlier [2] using $\eta(0,t) = R_0\sum_{n=1}^{\infty}(-1)^{n+1}n^{1/2}\{2n\gamma(L-\phi) + \frac{1}{2}\} \times e^{-2n\gamma\phi}$, where $R_0 = \frac{16}{3}\mathcal{E}_g\gamma_s^{3/2}(2\pi\cot\beta)^{1/2}/p_0^{1/4}$. Here, we compute the maximum runup of an N-wave (1) explicitly. We first note that the phase ϕ_m at the extremum runup satisfies $-\frac{4\gamma}{3}(L-\phi_m) = \sum_{n=1}^{\infty}(-1)^{n+1}n^{3/2}e^{-2n\gamma\phi_m}/[\sum_{n=1}^{\infty}(-1)^{n+1}n^{5/2}e^{-2n\gamma\phi_m}]$. Denoting $S(\phi_m) = \sum_{n=1}^{\infty}(-1)^{n+1}n^{3/2}e^{-2n\gamma\phi_m}$, we rewrite the equation for ϕ_m as $dS(\phi_m)/d\phi_m = 3S(\phi_m)/2(L-\phi_m)$. Solving for $S(\phi_m)$ for LDN $(L-\phi_m > 0)$, we find that $S(\phi_m) = S_0(L-\phi_m)^{-3/2}$. We then note that $-2\gamma\int S(\phi_m)d\phi_m = \sum_{n=1}^{\infty}(-1)^{n+1}n^{1/2}e^{-2n\gamma\phi_m}$ and obtain the maximum runup of a non-breaking leading-depression N-wave

$$\mathbf{R} = 3.3\mathcal{E}_g p_0^{1/4}Q(L,\gamma)\mathbf{R}_{\text{sol}}. \quad (6)$$

This relationship referred to as the N-wave runup law is valid when $4\gamma\cot\beta \gg 1$ for non-breaking LDN waves. The limiting wave amplitude for the validity of the above runup law can be obtained from the nonlinear shallow water theory using Carrier and Greenspan hodographic transformation [18] and is the same amplitude as outlined in [2] for $p_0 = 1$. $Q(L,\gamma)$ has to be determined numerically, but to the same order of approximation as (6) and over a wide range, Q varies linearly with L. We note that $\mathbf{R}_{\text{sol}}$ is the runup of a Boussinesq solitary wave of the same $\mathcal{H}$, and that (6) is asymptotically close to runup law for solitary waves given in [5]. This is reassuring; as Fig. 1(a) shows in the asymptotic limit LEN profiles describe solitary waves, for example when $L = 30$, $\mathcal{E}_g = 0.032$, $Q \approx 10$, and $p_0 = 1$; then (6) is almost identical to the runup law for solitary waves.

As examples, Figs. 3(a) and 3(b) show the variation of maximum runup with L and $\mathcal{H}$, respectively. Clearly in the region of physical interest the runup increases almost linearly with $\mathcal{H}$. It is shown elsewhere [2] that LDNs runup higher than LENs and solitary waves with the same leading wave height. Figure 4 shows the maximum runup variation with the crest-to-trough heights ratio; this parameter is uniquely determined from (1) through $\mathcal{H}$, L, and p_0. Notice that the maximum runup decreases from the isosceles N-wave limit to the solitary wave limit as the crest-to-trough ratio increases, consistent with the earlier observation that LDNs and LENs climb further than the equivalent solitary waves of the same $\mathcal{H}$ and steepness.

We have presented a model for the leading wave of tsunamis, encompassing as special cases waves similar to the Boussinesq solitary wave profiles, N-waves, and the certain combinations of Gaussian profiles [6]. The function can be fully described by specifying the crest amplitude $\mathcal{H}$, the steepness parameter p_0 and L, and it includes the individual classes of N-waves outlined in [2].

Our conjecture is that tsunamigenic faulting generates multilobe waves, and that the leading wave of the tsunami is important for estimating coastal effects, at least along open coastlines. Most physically realistic tsunamis retain their overall N-wave character even after transoceanic propagation. Near-shore–generated tsunamis do not have sufficient propagation distance to fully evolve, and their near-shore manifestation is almost invariably N-wave-like. We found that the maximum runup decreases as the ratio of trough height-to-crest height decreases. Hence,

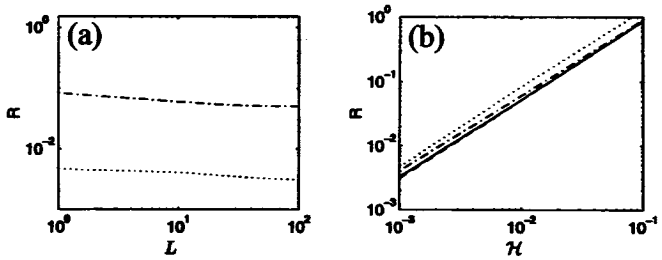

FIG. 3. $\mathbf{R}$ vs L for $\mathcal{H} = 0.001$ (··) and $\mathcal{H} = 0.1$ (− · −). (b) $\mathbf{R}$ vs $\mathcal{H}$ for $L = 1$ (··), $L = 10$ (− · −), $L = 50$ (—), and $L = 100$ (··).

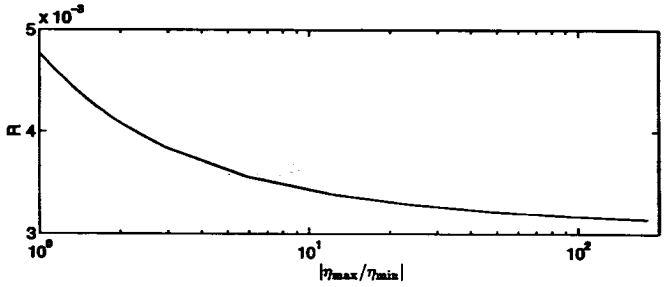

FIG. 4. Variation of maximum runup with peak-trough amplitude ratio for $\mathcal{H} = 0.001$, $L = 0 - 75$, $X_0 = 30$.

we conjecture that the dip angle [3,4] is important for runup calculations.

The two-dimensional character of the generation region or of the canonical solitary wave model notwithstanding, limits the application of our proposed model. We do note, however, that two-dimensional SW propagation models are still used extensively by oceanographers for calculating wave evolution and runup of wind-generated swell [19], a wave motion presumably much shorter than tsunamis. Nonetheless, we are reluctant to draw extensive physical conclusions other than claim that our initial profile provides a conceptual framework for analysis and for explaining certain field observations qualitatively, or even certain local numerical calculations as demonstrated in [3]. Yet we did perform simple calculations using our model in one of the recent tsunami catastrophes, where the coastal topography allowed it. One segment of the pacific coastline of Nicaragua is 73 km long with almost uniform plane beach slope ($\cot\beta = 33.18$), fronted by a continental shelf. This simplicity has allowed the use of two-dimensional numerical shoreline models coupled with three-dimensional offshore propagation models to calculate the runup and inundation. Figure 5 shows a comparison between the numerically generated surface profile for the Nicaraguan tsunami with that of Eq. (1) at the time when the wave

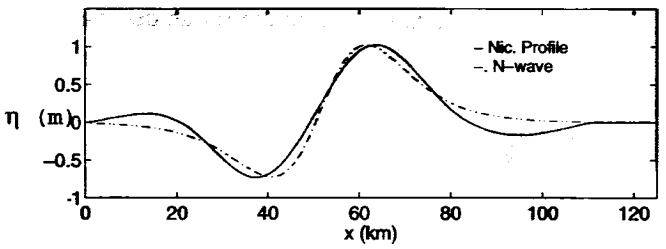

FIG. 5. Comparison of Nicaraguan tsunami profile at the toe of the beach using N-wave [Eq. (1)] with $L = 9$, $\mathcal{E}_g = 0.4823$, and $\gamma_s = 0.015$.

reaches the toe of the beach [20,21]. The measured and numerically computed maximum runup values were 6 ± 2 m, while the runup law (6) predicts 3.5 m. Our work further challenges the solitary wave profile paradigm as the standard model for tsunami runup and suggests that, particularly for near-shore tsunamis, the ground deformation, the maximum sea-bottom displacement, and the dip angle are of paramount importance in evaluating the coastal effects.

We are grateful for the generous support of the National Science Foundation (Cliff Astill, No. CMS 9201326) and for several useful discussions with Professor J. B. Keller, and Dr. Eric L. Geist. We are thankful to Vassili V. Titov for providing the Nicaraguan profile.

[1] L.-F. P. Liu, C. E. Synolakis, and H. Yeh, J. Fluid Mech. **229**, 675–688 (1991).
[2] S. Tadepalli and C. E. Synolakis, Proc. R. Soc. London Sect. A **445**, 99–112 (1994).
[3] E. Geist and S. Yoshioka, Nat. Hazards **13**, 151–177 (1996).
[4] T. Yamashita and R. Sato, J. Phys. Earth **22**, 415–440 (1974).
[5] C. E. Synolakis, J. Fluid Mech. **185**, 523–545 (1987).
[6] G. F. Carrier, in Proceedings of the IUGG/IOC International Tsunami Symposium, Wakayama, Japan, 1993.
[7] E. O. Tuck and Li-San Hwang, J. Fluid Mech. **51**, 440–461 (1972).
[8] G. F. Carrier, J. Fluid Mech. **24**, 641–659 (1966).
[9] G. Green, Trans. Cambridge Philos. Soc. 1838 (1837).
[10] H. Lamb, *Hydrodynamics* (Dover Publications Inc., New York, 1945).
[11] C. E. Synolakis, J. Waterw. Harbors Port Coastal Ocean Eng. **116**, 252–266 (1990).
[12] J. B. Keller and H. B. Keller, ONR Research Report No. NONR-3828(00), 1964, pp. 1–40.
[13] C. E. Synolakis, Phys. Fluids A **3**, 490–491 (1991).
[14] C. E. Synolakis and J. E. Skjelbreia, J. Waterw. Harbors Port Coastal Ocean Eng. **119**, 323–342 (1993).
[15] C. E. Synolakis, Q. Appl. Math. **46**, 105–107 (1988).
[16] S. Tadepalli and C. E. Synolakis, Q. Appl. Math. **51**, 103–112 (1994).
[17] M. Abramowitz and I. A. Stegun, *Handbook of Mathematical Functions* (Dover Publications Inc., New York, 1970).
[18] G. F. Carrier and H. P. Greenspan, J. Fluid Mech. **17**, 97–109 (1958).
[19] B. Raubenheimer *et al.*, J. Geophys. Res. **100**, 8751–8760 (1995).
[20] V. V. Titov and C. E. Synolakis, in Ref. [6], pp. 627–635.
[21] K. Satake, Pure Appl. Geophys. **144**, 455–470 (1995).